ESCUELA DE CONSTRUCCIÓN CIVIL
FACULTAD DE INGENIERÍA

Revista de la Construcción
Journal of Construction

Research Article

Feasibility study of using waste badminton string fibers in concrete by morphological, microstructural and tensile characteristics

Kumaresan M[1], Sindhu Nachiar S[2,*], Anandh Sekar[3]

[1] Department of Civil Engineering, SRM Institute of Science and Technology, College of Engineering and Technology, Kattankulathur (India); km1595@srmist.edu.in

[2] Department of Civil Engineering, SRM Institute of Science and Technology, College of Engineering and Technology, Kattankulathur (India); sindhus@srmist.edu.in

[3] Department of Civil Engineering, SRM Institute of Science and Technology, College of Engineering and Technology, Kattankulathur (India); anandhs@srmist.edu.in

*Correspondence: sindhus@srmist.edu.in

Received: 31.07.2023; **Accepted:**23.11.2023; **Published:** 29.12.2023

Citation: Kumaresan M., Sindhu S., and Anandh S. (2023). Feasibility study of using waste badminton string fibers in concrete by morphological, microstructural and tensile characteristics. Revista de la construcción. Journal of construction, 22(3), 694-708. https://doi.org/10.7764/RDLC.22.3.694.

Abstract: As the strings are cut off from the badminton racquet system, the whole string will be replaced with a new one and there is no other alternative. Hence those cut-off strings are considered as waste and cannot be recycled, tons of waste are retained as debris. Among many research on recycled synthetic fiber, this application of waste material is a new context in sustainable construction. Here five different samples are examined based on wide usage, recycled Waste Badminton String Fiber (WBSF) is characterized and physically examined using a Scanning Electron Microscope, Fourier Transform Infrared Spectroscopy, and X-ray diffraction to use it as a recycled synthetic fiber in various fiber reinforced concrete applications. The diameter and cross-sectional area of WBSF are studied using the Scanning Electron Microscope imaging technique and Image J application, which shows that the fiber is highly engineered with 3 layers namely elasticity outer, outer layer, and core fiber with the mean diameter and net cross-sectional area is 777.6 µm and 5,05,959 µm^2 respectively. The surface roughness of fiber is analyzed using ImageJ application which varies between 16-32 nm. The fiber samples are subjected to tensile loading the average tensile stress lies between 544.34 - 639.94 MPa. From the above examinations, the accurate diameter, net cross-sectional area, and voided area of the WBSF are calculated. The structural property and polymer relationship of the fiber are investigated using the X-ray diffraction technique and Fourier transform infrared spectroscopy, this reveals that the WBSF is of polyamide 6,6 form. The superior tensile stress compared to other recycled nylon fibers. So, the use of waste badminton string fiber in concrete is a new merging idea for fiber-reinforced concrete applications like pavements, pipes, tunnel lining, and other structural elements.

Keywords: Waste badminton string fiber, recycled synthetic fiber, microstructural study, concrete applications, polyamide 6,6.

1. Introduction

Throughout the past 30 years, many studies have been carried out on the use of recycled fibers as reinforcement in cementitious and polymer matrices (Kanan et al. 2022). As the commercial fiber cost is high and makes the composite uneconomical. The use of waste badminton string fiber (WBSF) is a new idea among several other recycled fibers (Spadea et al. 2015), the inclusion of emerging new fibers like optical cable (Suchorab, Franus, and Barnat-Hunek 2020), scrap nylon (Farooq et al. 2022), recycled steel wires (Pachideh and Gholhaki 2020) and glass fibers(Criado et al. 2015). These used badminton strings (WBSF) are stronger than other commercial nylon fibers in terms of tensile strength (M, Nachiar, and Sekar 2023).

To reinforce cement and polymer matrices, these WBSF can be utilized as discrete fibers. Usage of WBSF does not require any special treatment or processing before usage. So, the use of WBSF lowers the fiber cost in composites and fulfills environmental aspects (Kumaresan, Sindhu Nachiar, and Anandh 2022; M et al. 2023). The main significance is only 10% of strings are stressed in the sweet spot and if any one string is cut the total system is replaced by the new string. So, the remaining 90% of the strings in the racquet remain undisturbed (M et al. 2023). A total, of 10 kg of WBSF has been collected in a nearby sports shop for the investigation. Several stores in various parts of the world have noticed that these fibers are widely accessible for better purposes as they cannot be recycled.

Generally, the use of recycled synthetic fibers improves the toughness and impact resistance of composite materials. Moreover, it reduces shrinkage and post-cracking by acting as a bridge between the composite materials (Kumaresan et al. 2022)(Srimahachota et al. 2020). Hence, before incorporation into the composite, the physical and microstructural characteristics of this fiber should be investigated. The most accurate way to find the diameter and cross-sectional area of WBSF is by Scanning Electron Microscope (SEM). Although the diameter of the fiber is smaller than 0.8 mm, the accuracy of the SEM pictures is checked using ImageJ software. The voided area inside the fiber is also calculated and detected from the overall cross-sectional area of the fiber. The Fourier Transform Infrared Spectroscopy (FTIR) is analyzed for all the test samples and observed the band associated with each peak and its bond interface observance. The X-Ray diffraction (XRD) is used to know the polymer structure of various samples and their polymeric differences.

Table 1. Physical and mechanical properties of new fiber and old fiber (m et al. 2023)

Fiber sample	Mean diameter (μm)	Net cross-sectional Area (μm^2)	Tensile strength ASTM C1557 (MPa)	Tensile modulus ASTM C1557 (MPa)	Density (kg/m^3)
New fiber	799.1	504,786.3	621±86	4870	1100
Old fiber	776.3	498,125.0	550±75	4843	1100

Kumaresan et al (M et al. 2023) have investigated the physical and mechanical properties of old and new fibers of a single manufacturer given in Table 1. However, here the study is made on waste badminton string fibers from five different leading manufacturers considered based on a wide range of usage in badminton forums. Those samples taken for investigation are named as Sample A, Sample B, Sample C, Sample D, and Sample E. The tensile properties of these fiber samples are tested as per ASTM C1557(ASTM C1557).

The research signifies the global challenge of waste management by reusing discarded badminton string fibers (WBSF). The incorporation of WBSF in concrete could offer a cost-effective alternative for construction materials. This has the potential to reduce expenses associated with conventional fiber reinforcement materials, making construction more economically viable. The specific focus on waste badminton string fibers is a material that has not been extensively explored in the context of construction materials. This unique approach distinguishes the research from earlier works on recycled fibers. The detailed microstructural analysis using (SEM), (FTIR), and (XRD) provides a comprehensive understanding of the composition and the properties of WBSF. This thorough examination adds a novel dimension to the study. The practical application of this work lies in promoting sustainability in the construction industry by utilizing recycled materials which is not limited to concrete pipes, tunnel lining segment, and structural elements.

2. Experimental methods

SEM (Paiva 2007), FTIR (Madhu et al. 2019),and XRD (Khan et al. 2021) are used for the morphological and microstructural investigation to find the properties of different samples of WBSF. Further, these fiber samples are subjected to a tensile loading. All the parameters are compared with the previous work in this area. The flowchart of the study is shown in Figure 1.

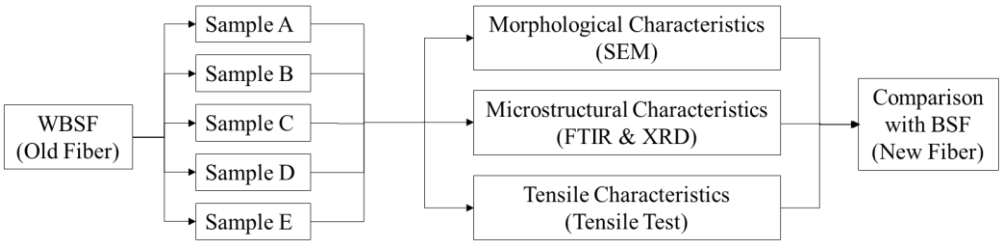

Figure 1. Flowchart of methodology.

The samples from different manufacturers, and WBSF samples undergone a thorough microstructural examination. The SEM imaging technique played a crucial role in determining the diameter and area of each sample with precision. Furthermore, FTIR and XRD were employed to unravel the material characteristics of all five samples. The comparison and discussion of results highlighted show the differences and similarities among the samples. Importantly, the study concluded with a comparative analysis between WBSF samples and new fibers, providing insights between them.

2.1. *Morphological characteristics*

The thermoscientific apreo a scanning electron microscope (SEM) was employed to assess the morphological properties of multifilament Waste Badminton String Fiber (WBSF). Initially, the samples underwent a cleaning process with distilled water, followed by dehydration at atmospheric temperature. Subsequently, the prepared samples were subjected to SEM imaging at magnifications ranging from 150x to 8000x. To gain insights into the internal layers of the fiber, a lengthwise slicing technique was applied to the top surface of the WBSF. This method allowed for a thorough examination of the three distinct layers – elasticity outer, outer layer, and core fiber. For precise measurements of diameter and area, the fiber was further sliced perpendicularly using a sharp cutting edge, ensuring accurate characterization of WBSF morphology (Maria, Bertelsen, and Ottosen n.d.). Here ImageJ software application is used to understand the fiber surface roughness for all the samples(Hilal 2021).

2.2. *Microstructural characteristics*

The microstructural characteristics of WBSF is examined using FTIR and XRD, the FTIR spectrum serves as a detailed blueprint. The diverse bands in the FTIR spectrum enable the observation and characterization of substances of newfound interest. For this purpose, the Shimadzu IR Tracer-100 FTIR spectrometer, known for its integrated automated dehumidifier and impressive 4 cm^{-1} resolution, was employed to capture the infrared spectra. This spectroscopic method allows for a thorough examination of molecular vibrations and functional groups, providing essential information for material characterization. The utilization of advanced instrumentation ensures the accuracy and reliability of the gathered spectra, enhancing the scientific rigor of the study (Vasanthan and Salem 2001).

An integral component of the experimental methodology involved X-ray diffraction (XRD) analysis, aimed at unraveling the polymorphic structure inherent in the material. XRD is a robust analytical tool renowned for its capability to discern the arrangement of atoms within the crystal lattice of a substance. In this context, it served as a key instrument for identifying and characterizing different crystal forms or polymorphs present in the material under investigation. Commonly encountered in polymers are the α-monoclinic form and the γ-monoclinic form, two distinct crystal structures that were explored in this study. The findings from XRD contribute significantly to the understanding of the material's structural properties and lay the groundwork for further analysis (Mohammadhosseini, Tahir, and Sayyed 2018).

2.3. *Tensile charactertistics*

All fiber samples have undergone tensile testing in accordance with ASTM C1557 (ASTM C1557) to observed the tensile characteristics of WBSF. The experimental setup and fiber arrangement are shown in Figure 2. The fiber samples were positioned between aluminum plates, ensuring a gauge length of 100 mm to prevent slippage during the test. To prevent fiber compression during specimen clamping, a rigid adhesive glue was applied between the aluminum plates.

The tensile strength tests were conducted using a universal testing machine with computer control capabilities. The testing machine maintained a rate of strain of 2 mm/min throughout the experiment. A load cell with a capacity of 250 kg was employed to measure and record the results. The computerized system allowed for direct extraction of data, providing precise and efficient monitoring of the tensile strength performance of each fiber sample. This comprehensive testing approach ensures an accurate evaluation of the tensile properties of the fibers. The rigid adhesive and gauge length specifications contribute to the integrity of the testing process by minimizing potential sources of error, such as slippage or compression, and the computer-controlled system further enhances the precision of data collection.

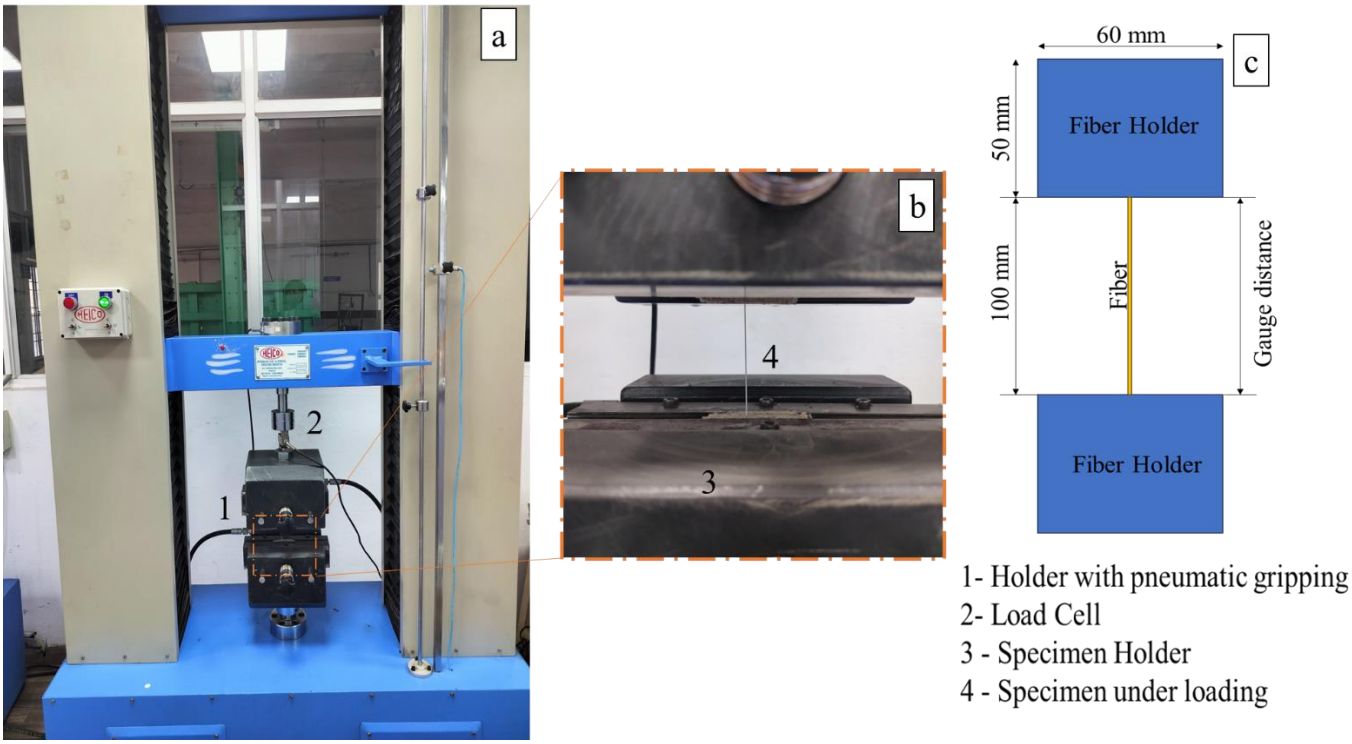

Figure 2. Test setup (a) universal Testing Machine (b) specimen gripping system (c) schematic representation of test specimen.

3. Experimental results and analysis

The findings obtained from morphological, microstructural and tensile characteristics of WBSF samples from five distinct manufacturers, are elaborated upon in this section. The section provides a detailed discussion of the outcomes derived from the examination of WBSF samples. The investigation of the fiber's physical attributes via SEM, the functional response from FTIR technique, and the analysis of polymorphic structures through XRD. The comparison and interpretation of these results contribute to a comprehensive understanding of the microstructural characteristics exhibited by WBSF samples from diverse sources.

3.1. Morphological characteristics

As shown in Figure 3, the SEM image of the fibers shows three unique layers namely elasticity outer which is the outer layer, and outer layer which protects the core fiber, and the inner core fiber which is compressed of more than 350 monofilaments for all the five samples (M et al. 2023). These fibers experience more strain and impact before being torn from the racquet system. These three layers of fibers provide support for enduring the extreme stress caused due to stretching.

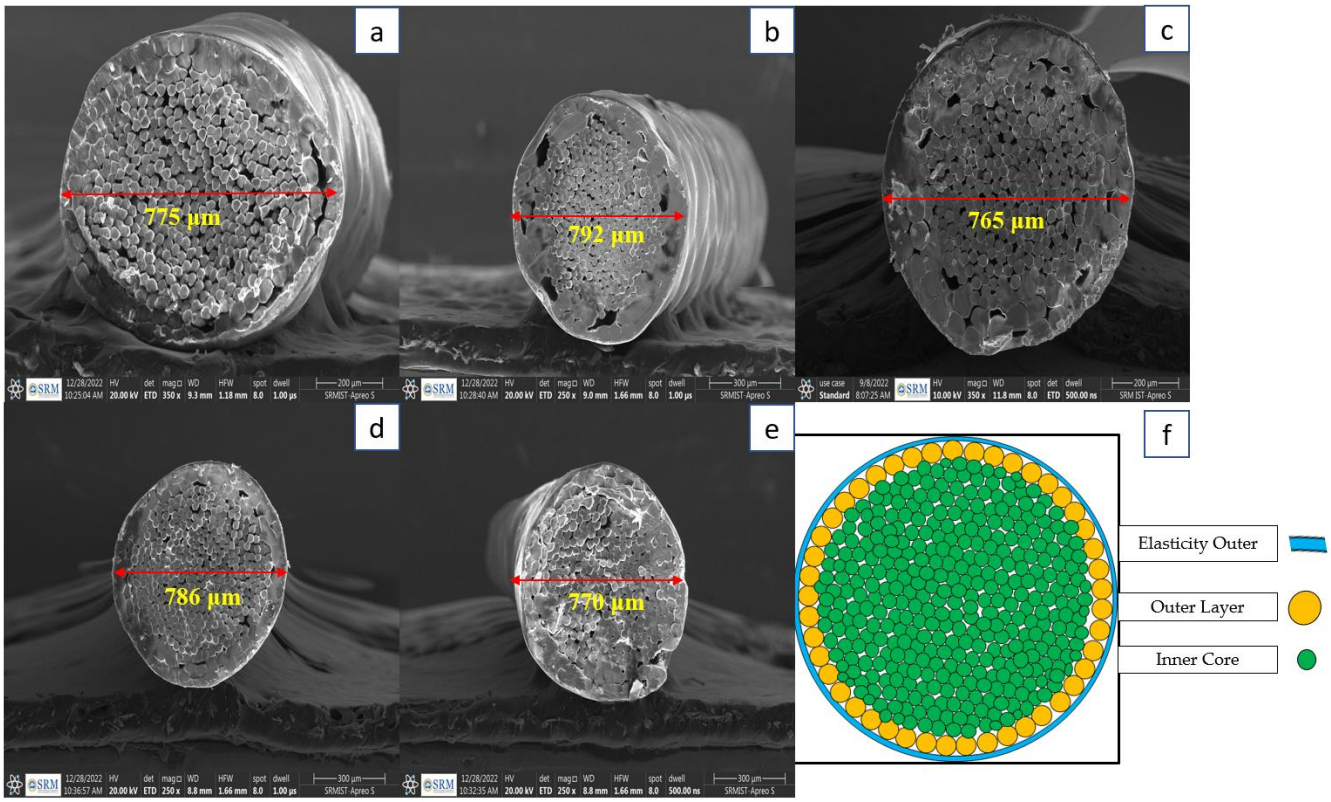

Figure 3. Diameter of WBSF using SEM Image (a) sample A (b) sample B (c) sample C (d) sample D (e) sample E (f) schematic diagram of WBSF.

Table 2. Dimensions of different layers of WBSF.

Fiber layers	Sample A (SD)	Sample B (SD)	Sample C (SD)	Sample D (SD)	Sample E (SD)
Outer layer ϕ (µm)	55 (2.5)	52 (3.2)	46 (2.0)	50 (3.1)	53 (1.9)
Core fiber ϕ (µm)	23 (0.6)	25 (0.8)	21 (0.5)	24 (0.9)	22 (0.7)
Elasticity outer t (µm)	15 (5.0)	25 (8.0)	19 (4.0)	21 (6.0)	18 (5.0)

ϕ – Diameter, t – Thickness, SD – Standard Deviation

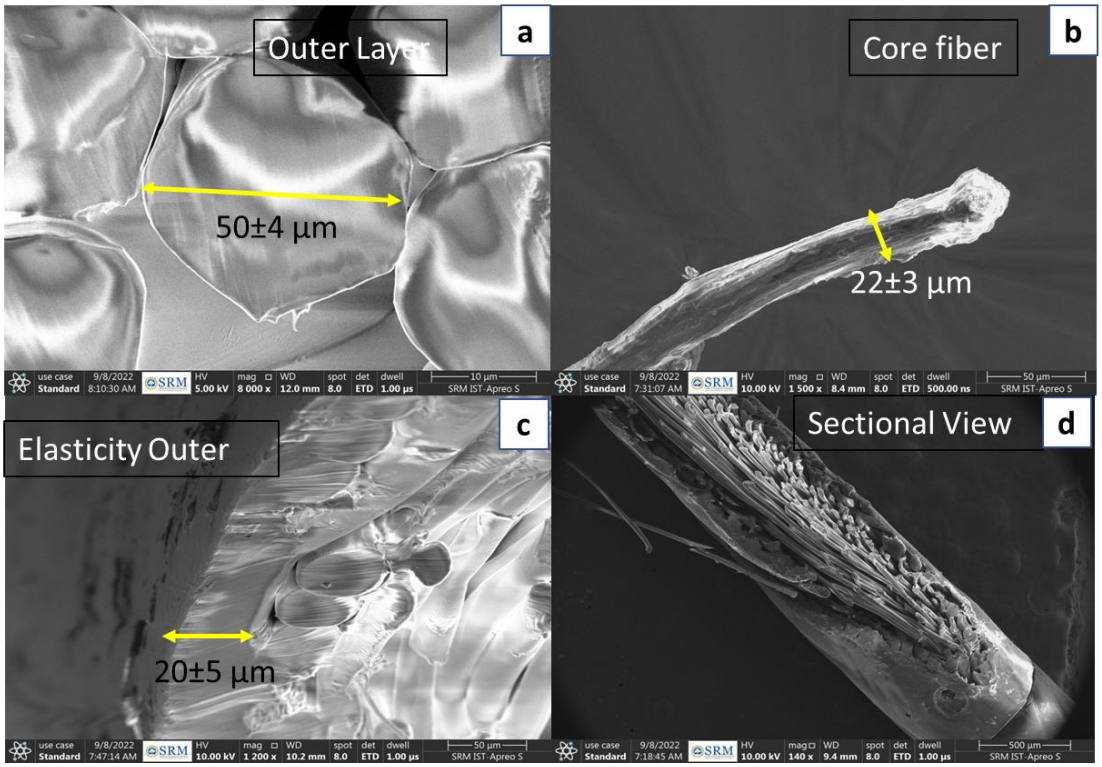

Figure 4. SEM image of WBSF (a) outer layer (b) core fiber (c) elasticity outer (d) sectional view.

The whole fiber system is of a non-uniform circular shape. The microfibers present in the outer layer and the core fiber is also of non-uniform circular shape. Figure 4 depicts a close-up of the microfibers' placement within the core and outer layers (Mazzoli, Monosi, and Plescia 2015). ImageJ software is used to describe the fiber's diameter and area (Gopinath, Senthilkumar, and Babu 2018; Munawar, Umemura, and Kawai 2007). In order to accomplish the SEM Imaging procedure, three separate sample fibers are cut precisely perpendicularly and held vertically. The area is found by using ImageJ software by plotting the boundaries on the outer of the fiber. The mean diameter of the WBSF is 777 µm. The overall area of WBSF is calculated from Image J software by setting the exact scaling and the boundary is marked as shown in Figure 5. The net cross-sectional area is obtained by detecting the voided area as shown in Figure 6. The black shots are the voided area obtained from the threshold method from Image J software. The average net area of fibers is 4,89,909 μm^2. There is no much difference observed in the diameter and area of different samples of fibers. The mean diameter and the cross-sectional area of fibers are tabulated in Table 3. The dimensions of elasticity outer, outer layer, and core fiber are tabulated in Table 2.

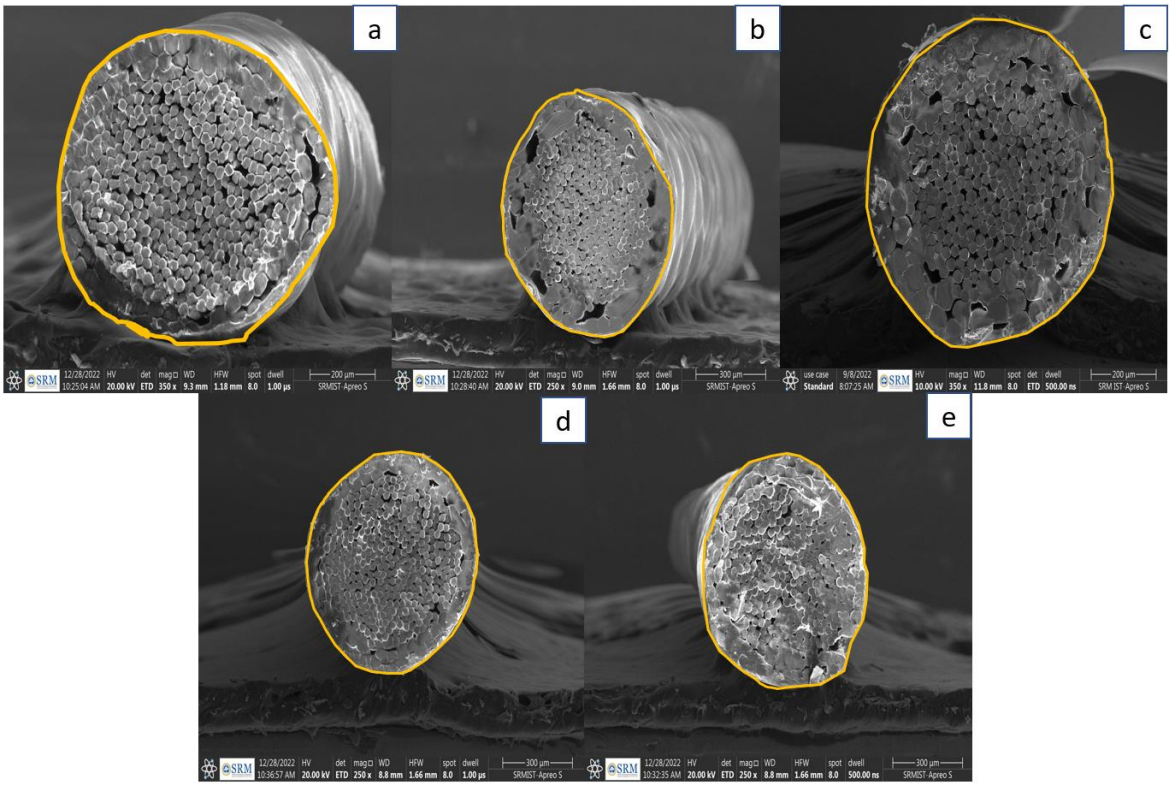

Figure 5. Area of WBSF (a) sample A (b) sample B (c) sample C (d) sample D (e) sample E.

Table 3. Mean diameter and cross-sectional area of various samples of WBSF.

Fiber sample	Mean diameter (μm)	Standard deviation of diameter (μm)	Overall cross-sectional area of the fiber (μm^2)	Area of voids of the fiber (μm^2)	Net area of the fiber (μm^2)
A	775	12	5,01,550	3056	4,98,494
B	792	9	5,01,130	2850	4,98,280
C	765	23	4,83,261	3760	4,79,501
D	786	11	4,90,255	2350	4,87,905
E	770	15	4,89,022	3657	4,85,365
Average	777	14	4,93,044	3,135	4,89,909

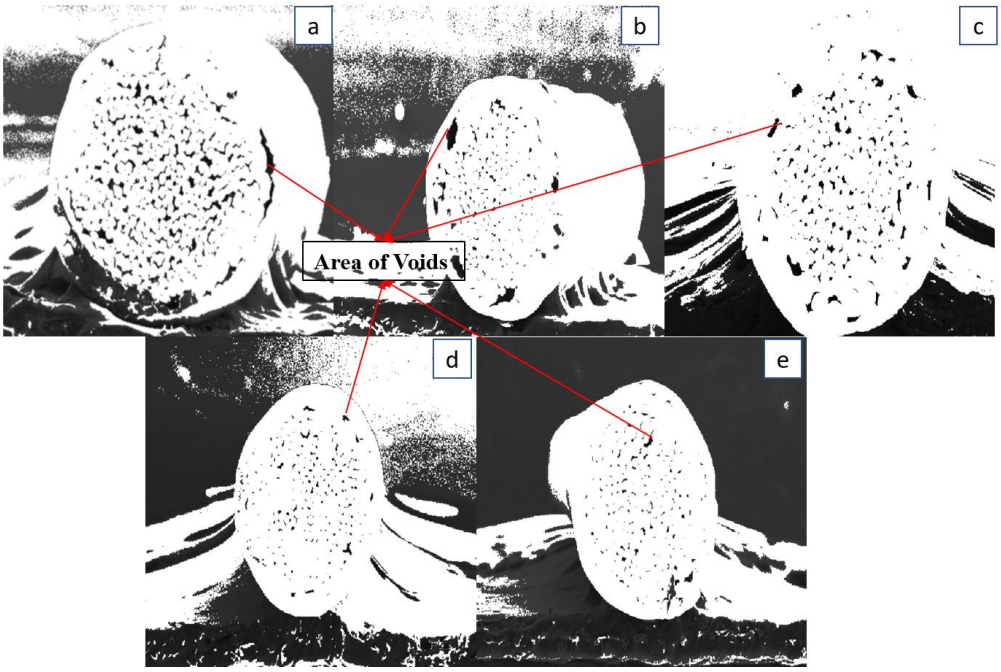

Figure 6. Area of voids (a) sample A, (b) sample B, (c) sample C, (d) sample D, and (e) sample E.

The surface roughness of the fibers plays a crucial role in influencing the bond characteristics between the fibers and the composite matrix. To evaluate this parameter, SEM images of all five samples were analysed using the ImageJ application(Naik et al. 2019). Each sample was scanned uniformly, and the scan length is illustrated in Figure 7. The obtained surface roughness values for all samples are presented in Figure 8.

The SEM images, processed through the ImageJ application, allowed for a detailed examination of the fiber surfaces. The scan length depicted in Figure 8 ensures a comprehensive analysis of the entire sample, capturing variations in surface characteristics. Figure 8 illustrates the surface roughness data for each of the five samples. The variations in roughness values provide insights into the texture and irregularities present on the fiber surfaces. A higher surface roughness indicates a more textured and uneven fiber surface, which can contribute to improved bonding with the composite matrix(Antonova et al. 2021).

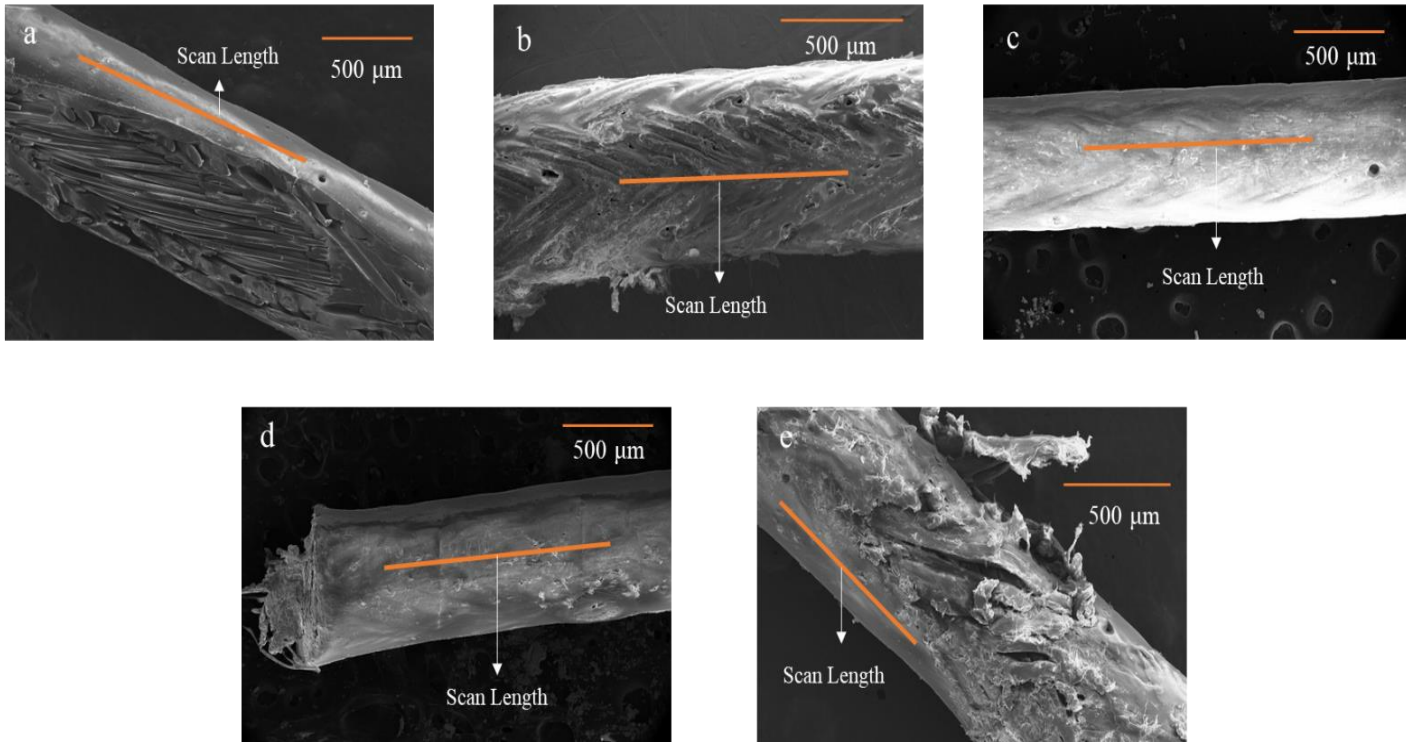

Figure 7. Surface roughness (a) sample A, (b) sample B, (c) sample C, (d) sample D, and (e) sample E.

The maximum surface roughness is observed in sample B followed by sample A, sample C, sample E, and sample D. The maximum surface roughness is recorded as 28, 32, 27, 16, and 17 nm for sample A, sample B, sample C, sample D, and sample E respectively. More waviness is observed for sample B, all other samples have almost similar patterns of waviness on the surface fiber. Here the surface roughness of WBSF samples varies between 16-32 nm as shown in Figure 8.

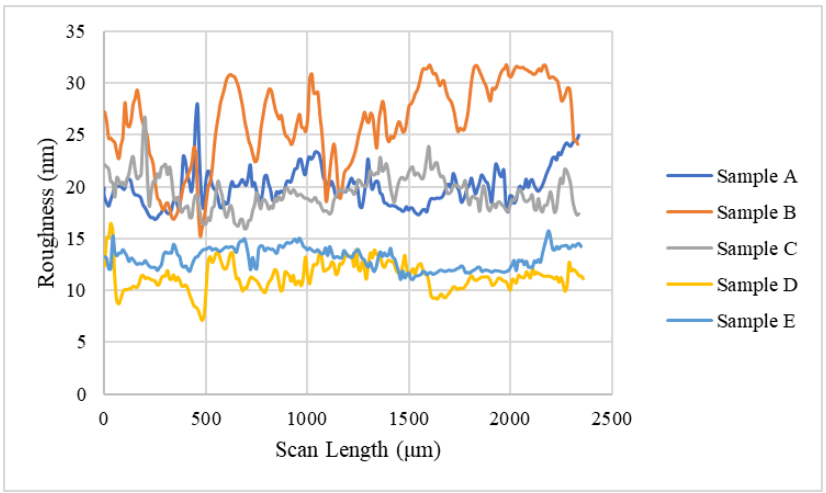

Figure 8. Surface roughness of the fiber.

3.2. Microstructural characteristics

The peak position 1 range between 3290-3295 cm-1 applies the N-H stretch of the amino group (Vasanthan and Salem 2001), while the peak position 2 ranges between 2920-2845 cm-1 represents the vibration of CH2 asymmetric and symmetric stretch, respectively, according to the FTIR band data. The two distinct peaks at peak positions 4 and 5 range between 1630-1635 and 1540-1545 cm-1 respectively signify the amide I and II bands (Vasanthan 2012). The C=O stretch is visible in the peak measured at 1760 and 1665 cm-1. However, in this instance, the peak for the C=O stretch is measured at 1635 cm-1 because the amino I group's interaction with the hydrogen bond is the main observation. The amide II band peak emerges at 1545 cm-1 as a result of the N-H stretch. Figure 9 displays the band assignment and absorbance pattern for all the samples, the above absorbance of WBSF reveals the samples are the purest form of polyamide 6,6 (Fornes and Paul 2003; Vasanthan and Salem 2001).

Table 4. FTIR band assignment of various samples of WBSF.

Peak position	Band position/cm^{-1}					Range	Assignments
	Sample A	Sample B	Sample C	Sample D	Sample E		
1	3291	3290	3295	3294	3291	3330-3250	N-H stretching
2	2922	2923	2920	2920	2921	3000-2840	Asymmetric C-H stretching
3	2851	2856	2850	2845	2850	3000-2840	Symmetric C-H stretching
4	1635	1630	1632	1630	1631	1730-1600	C=O stretching
5	1545	1542	1540	1545	1541	1500-1550	N-H stretch
6	1464	1460	1463	1465	1460	1400-1500	CH_2 scissors
7	1262	1260	1265	1260	1261	1250-1300	CH_2 twist-wagging
8	720	720	723	721	720	720-750	N-H deformation

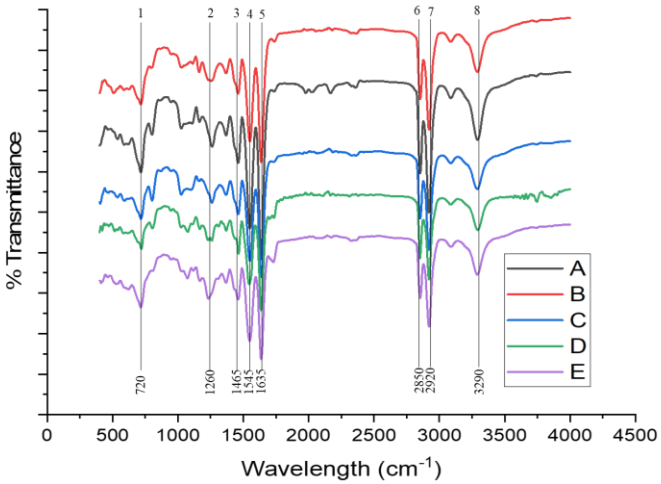

Figure 9. FTIR of various samples of WBSF.

Generally, polyamide shows the α and γ crystalline phases depending on the crystalline conditions. Here, the two intense peaks at 2θ= 20° and 23° are absorbed in the XRD pattern. This leads to the observation of the α-crystalline form in the peak range of 19.79°-20.11° and the γ-crystalline form in the two high-intensity peaks ranges from 2θ = 19.79°-20.11° and 23.23°-23.66° (Fornes and Paul 2003). These findings show that the WBSF of all samples is of the purist form of polyamide 6,6's crystalline structure, as shown in Figure 10.

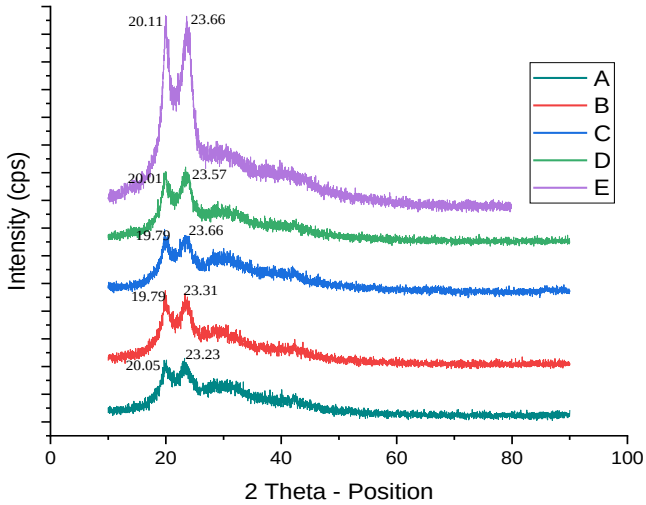

Figure 10. XRD of various samples of WBSF.

3.3. Tensile characteristics

The tensile stress for all five samples is expressed with the average of three successful test specimen results. The average tensile stress (σ_{Avg}) is 555.33, 635.05, 609.83, 639.94, and 544.34 MPa is obtained for Sample A, Sample B, Sample C, Sample D, and Sample E respectively as shown in Figure 11. Among all the samples Sample D has a high tensile strength of 639.94 MPa. The maximum and minimum tensile strength lies between 544.34 and 639.94 MPa respectively. In some of the specimen results there is sudden slip in the graph is observed, this is due to the failure of the outer layers of the fiber. The ultimate failure is observed after the failure of the core fiber. The strain value of the fiber lies between 0.15 to 0.4, the high strain values represent the ductility of the material, in specific Sample D specimens are more ductile compared to

other samples. The linear trend is observed for all the samples shows the ability to retain its elasticity until the ultimate failure of the specimen. The obtained tensile stress and strain values are higher when compared to other recycled nylon fibers(Fashandi, Pakravan, and Latifi 2019; Maria et al. n.d.; Park, Kim, and Kim 2020).

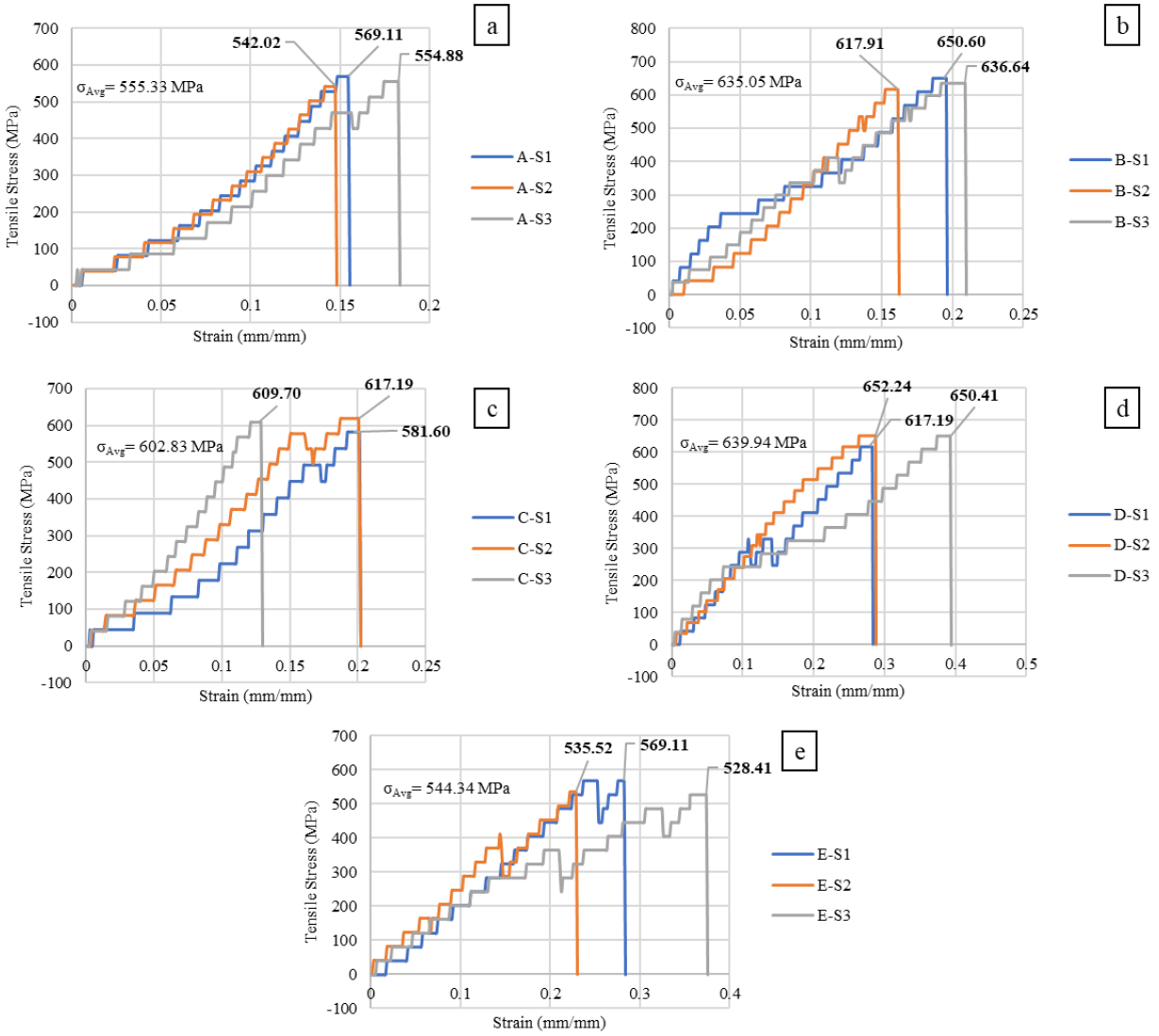

Figure 11. Tensile stress vs strain graph (a) sample A (b) sample B (c) sample C (d) sample D (e) sample E.

4. Comparison of WBSF properties with BSF

The comparison of BSF (Badminton String Fiber) and WBSF gives the difference in properties, to easily analyze. Kumaresan et al.,(M et al. 2023), have investigated the microstructural and mechanical properties of BSF, which is compared with all the five samples tabulated in Table 5. From the SEM image the diameter, net cross-sectional area, and voided area of the new fiber is higher when compared to the old fibers. Because the BSF are not stressed whereas the old fibers are stressed and stretched to induce tension in the badminton racquet system. The FTIR and XRD results of all the fibers (BSF and WBSF) confirm the composition and presence of polyamide 6,6. The tensile characteristics shows the difference between the five different samples and with BSF.

Table 5. Comparison of WBSF properties with BSF.

Fiber characteristics		BSF(Met al. 2023)	WBSF					
			Sample A	Sample B	Sample C	Sample D	Sample E	Average (WBSF)
Morphological	Diameter(μm)	799	775	792	765	786	770	777
	net cross sectional area (μm^2)	504786	498494	498280	479501	487905	485365	489909
	voided area (μm^2)	4684	3056	2850	3760	2350	3657	3135
Chemical	Functionalgroup Response confirms	Polyamide 6,6	Polyamide 6,6	Polyamide6,6	Polyamide 6,6	Polyamide 6,6	Polyamide 6,6	Polyamide 6,6
	polymeric structure confirms	Polyamide 6,6	Polyamide 6,6	Polyamide6,6	Polyamide 6,6	Polyamide 6,6	Polyamide 6,6	Polyamide 6,6
Tensile	Average tensile stress (MPa)	648.53	555.33	635.05	609.83	639.94	544.34	596.89

5. Conclusion

The morphological, microstructural, and tensile characteristics of WBSF samples from five different manufacturers have been investigated. The study's findings are the following:

1. The mean diameter and net cross-sectional area of the WBSF are 777 μm and 489909 μm^2 respectively. The diameter and net cross-sectional area of WBSF is 3% less compared to BSF.
2. The surface roughness of WBSF lies between the range of 16-32 nm, which is higher compared to other nylon fibers.
3. From the XRD and FTIR observation, all the samples of WBSF are found to have the purest composition of polyamide 6,6. Shows the same chemical composition is used in the manufacturing of all the fibers.
4. The average tensile strength of the WBSF samples lies between 544.34 – 639.94 MPa, which is higher compared to other recycled nylon fibers.
5. The average tensile strength of WBSF is 596.89 MPa, which is 8% less when compared to the average tensile strength of BSF (648.53 MPa)
6. There is no significant difference is observed between the values of WBSF and BSF. The material composition and fiber tensile property is almost similarly maintained by the leading manufacturers.

So, the use of any WBSF would be a better idea to investigate the viability of integrating WBSF in epoxy polymer and the cementitious matrix. Tough among all, only five samples are considered for the study. Extending, the consideration of temperature variations in fiber can be studied.

Author contributions: Conceptualization and methodology, writing—original draft preparation, Kumaresan M; validation, editing and supervision, S Sindhu Nachiar.; data curation and supervision, Anandh Sekar.; All authors have read and agreed to the published version of the manuscript.

Funding: This research received no external funding.

Acknowledgments: We acknowledge the XRD FACILITY at SRMIST setup with support from MNRE (Project No. 31/03/2014-15/PVSE-R&D), Government of India. We acknowledge SRMIST for the high-resolution scanning electron microscopy (HR-SEM) facility and Fourier transform infrared spectroscopy (FTIR).

Conflicts of interest: The authors declare no conflict of interest.

References

Antonova, Anna, Marika Eik, Ville Jokinen, and Jari Puttonen. 2021. "Effect of the Roughness of Steel Fibre Surface on Its Wettability and the Cement Paste Close to Fibre Surface." *Construction and Building Materials* 289:123139. doi: 10.1016/j.conbuildmat.2021.123139.

ASTM C1557−14; Standard Test Method for Tensile Strength and Young's Modulus of Fibers. ASTM International: West Conshohocken, PA, USA, 2015.

Criado, M., I. García-díaz, J. M. Bastidas, F. J. Alguacil, F. A. López, and C. Monticelli. 2015. "Effect of Recycled Glass Fiber on the Corrosion Behavior of Reinforced Mortar." *Construction and Building Materials* 64(2014):261–69. doi: 10.1016/j.conbuildmat.2014.04.049.

Farooq, Muhammad Ahmad, Muhammad Fahad, Babar Ali, Shahid ullah, Mohamed Hechmi El Ouni, and Ahmed Babeker Elhag. 2022. "Influence of Nylon Fibers Recycled from the Scrap Brushes on the Properties of Concrete: Valorization of Plastic Waste in Concrete." *Case Studies in Construction Materials* 16(March):e01089. doi: 10.1016/j.cscm.2022.e01089.

Fashandi, Hossein, Hamid Reza Pakravan, and Masoud Latifi. 2019. "Application of Modified Carpet Waste Cuttings for Production of Eco-Efficient Lightweight Concrete." *Construction and Building Materials* 198:629–37. doi: 10.1016/j.conbuildmat.2018.11.163.

Fornes, T. D., and D. R. Paul. 2003. "Crystallization Behavior of Nylon 6 Nanocomposites." *Polymer* 44(14):3945–61. doi: 10.1016/S0032-3861(03)00344-6.

Gopinath, Ajith, M. Senthilkumar, and Avinash Babu. 2018. "Evaluation of Mechanical Properties and Microstructure of Polyester and Epoxy Resin Matrices Reinforced with Jute, E-Glass and Coconut Fiber." *Materials Today: Proceedings* 5(9):20092–103. doi: 10.1016/j.matpr.2018.06.376.

Hilal, Ameer A. 2021. "Effect of Aggregate Roughness on Strength and Permeation Characteristics of Lightweight Aggregate Concrete." *Journal of Engineering (United Kingdom)* 2021. doi: 10.1155/2021/9505625.

Kanan, Mohammad, Bechir Wannassi, Ahmad S. Barham, Mohamed Ben Hassen, and Ramiz Assaf. 2022. "The Quality of Blended Cotton and Denim Waste Fibres: The Effect of Blend Ratio and Waste Category." *Fibers* 10(9). doi: 10.3390/fib10090076.

Khan, Anish, R. Vijay, D. Lenin Singaravelu, M. R. Sanjay, Suchart Siengchin, Francis Verpoort, Khalid Ahmad Alamry, and Abdullah M. Asiri. 2021. "Characterization of Natural Fibers from Cortaderia Selloana Grass (Pampas) as Reinforcement Material for the Production of the Composites." *Journal of Natural Fibers* 18(11):1893–1901. doi: 10.1080/15440478.2019.1709110.

Kumaresan, M., S. Sindhu Nachiar, and S. Anandh. 2022. "Implementation of Waste Recycled Fibers in Concrete: A Review." *Materials Today: Proceedings* 68:1988–94. doi: 10.1016/j.matpr.2022.08.228.

M, Kumaresan, S. Sindhu Nachiar, and Anandh Sekar. 2023. "Engineering Properties of Waste Badminton String Fiber." *Fibers* 11(3):25. doi: 10.3390/fib11030025.

Madhu, P., M. R. Sanjay, P. Senthamaraikannan, S. Pradeep, S. S. Saravanakumar, and B. Yogesha. 2019. "A Review on Synthesis and Characterization of Commercially Available Natural Fibers: Part II." *Journal of Natural Fibers* 16(1):25–36. doi: 10.1080/15440478.2017.1379045.

Maria, Ida, Gieysztor Bertelsen, and Lisbeth M. Ottosen. n.d. *Engineering Properties of Fibres from Waste Fishing Nets Materials, Systems and Structures in Civil Engineering Circular Ocean*.

Mazzoli, Alida, Saveria Monosi, and Eleonora Stella Plescia. 2015. "Evaluation of the Early-Age-Shrinkage of Fiber Reinforced Concrete (FRC) Using Image Analysis Methods." *Construction and Building Materials* 101:596–601. doi: 10.1016/j.conbuildmat.2015.10.090.

Mohammadhosseini, Hossein, Mahmood Md Tahir, and M. I. Sayyed. 2018. "Strength and Transport Properties of Concrete Composites Incorporating Waste Carpet Fibres and Palm Oil Fuel Ash." *Journal of Building Engineering* 20:156–65. doi: 10.1016/j.jobe.2018.07.013.

Munawar, Sasa Sofyan, Kenji Umemura, and Shuichi Kawai. 2007. "Characterization of the Morphological, Physical, and Mechanical Properties of Seven Nonwood Plant Fiber Bundles." *Journal of Wood Science* 53(2):108–13. doi: 10.1007/s10086-006-0836-x.

Naik, Dayakar L., Achintyamugdha Sharma, Rajender Reddy Chada, Ravi Kiran, and Todd Sirotiak. 2019. "Modified Pullout Test for Indirect Characterization of Natural Fiber and Cementitious Matrix Interface Properties." *Construction and Building Materials* 208:381–93. doi: 10.1016/j.conbuildmat.2019.03.021.

Pachideh, Ghasem, and Majid Gholhaki. 2020. "An Experimental Study on the Performance of Fine-Grained Concrete Incorporating Recycled Steel Spring Exposed to Acidic Conditions." *Advances in Structural Engineering* 23(11):2458–70. doi: 10.1177/1369433220915794.

Paiva, M. C. 2007. "SCIENCE AND Alfa Fibres : Mechanical , Morphological and Interfacial Characterization." 67:1132–38. doi: 10.1016/j.compscitech.2006.05.019.

Park, Jun Kil, Min Ook Kim, and Dong Joo Kim. 2020. "Pullout Behavior of Recycled Waste Fishing Net Fibers Embedded in Cement Mortar." *Materials* 13(18). doi: 10.3390/MA13184195.

Spadea, Saverio, Ilenia Farina, Anna Carrafiello, and Fernando Fraternali. 2015. "Recycled Nylon Fibers as Cement Mortar Reinforcement." *Construction and Building Materials* 80:200–209. doi: 10.1016/j.conbuildmat.2015.01.075.

Srimahachota, Teeranai, Haruka Matsuura, Shun Yamaguchi, and Hiroshi Yokota. 2020. "Influences of Nylon Fiber Geometries and Contents on Mechanical Behavior of Reinforced Mortar." *Journal of Asian Concrete Federation* 6(2):14–23. doi: 10.18702/acf.2020.12.6.2.14.

Suchorab, Zbigniew, Malgorzata Franus, and Danuta Barnat-Hunek. 2020. "Properties of Fibrous Concrete Made with Plastic Optical Fibers from E-Waste." *Materials* 13(10):1–25. doi: 10.3390/ma13102414.

Vasanthan, N. 2012. "Crystallinity Determination of Nylon 66 by Density Measurement and Fourier Transform Infrared (FTIR) Spectroscopy." 16–19.

Vasanthan, N., and D. R. Salem. 2001. "FTIR Spectroscopic Characterization of Structural Changes in Polyamide-6 Fibers during Annealing and Drawing." (August 2000):536–47.